response. In this context, repression of T-cell activation may impede long-term cell survival in the rudimentary immune environment of immunodeficient animals. Second, the immunosuppressive properties of mAb 2E1 offer a new potential alternative for target manipulation of the immune response *in vivo*. The xenochimaeric system used here is the closest known model to mimic widespread human diseases such as GVH and EBV-induced lymphomagenesis. Advanced derivatives of mAb 2E1, or synthetic antagonists of this new co-stimulatory pathway, may be beneficial for *in vivo* immunosuppression in humans. □

Received 24 November 1995; accepted 17 January 1996.

1. Davie, E. W., Fujikawa, K. & Kisiel, W. *Biochemistry* **30,** 10363–10370 (1991).
2. Patthy, L. *Cell* **41,** 657–663 (1985).
3. Vu, T.-K. H., Hung, D. T., Wheaton, V. I. & Coughlin, S. R. *Cell* **64,** 1057–1068 (1991).
4. Stitt, T. N. *et al. Cell* **80,** 661–670 (1995).
5. Glenn, K. C. & Cunningham, D. D. *Nature* **278,** 711–718 (1979).
6. Gasic, G. P., Arenas, C. P., Gasic, T. B. & Gasic, G. J. *Proc. natn. Acad. Sci. U.S.A.* **89,** 2317–2320 (1992).
7. Ross, R. *Nature* **362,** 801–809 (1993).
8. Altieri, D. C. *J. biol. Chem.* **269,** 3139–3142 (1994).
9. Altieri, D. C. & Stamnes, S. J. *Cell. Immun.* **155,** 372–383 (1994).
10. Rothman, B. L. *et al. J. Immun.* **147,** 2493–2499 (1991).
11. Merkenschlager, M., Buck, D., Beverley, P. C. & Sattentau, Q. *J. Immun.* **145,** 2839–2845 (1990).
12. Walker, C., Bettens, F. & Pichler, W. J. *Eur. J. Immun.* **17,** 873–880 (1987).
13. Mosier, D. E., Gulizia, R. J., Baird, S. M. & Wilson, D. B. *Nature* **335,** 256–259 (1988).
14. Mosier, D. E., Gulizia, R. J., Baird, S. M. & Wilson, D. B. *Nature* **338,** 211 (1989).
15. Mosier, D. E., Gulizia, R. J., Torbett, B. E., Baird, S. M. & Wilson, D. B. *Nature* **353,** 509 (1991).
16. Duchosal, M. A., Eming, S. A., McConahey, P. J. & Dixon, F. J. *Am. J. Path.* **141,** 1097–1113 (1992).
17. Pirruccello, S. J. *et al. Am. J. Path.* **140,** 1187–1194 (1992).
18. Veronese, M. L. *et al. J. exp. Med.* **176,** 1763–1767 (1992).
19. Mosier, D. E. *et al. Curr. Topics Microbiol. Immun.* **152,** 195–199 (1989).
20. Okano, M. *et al. Am. J. Path.* **137,** 517–522 (1990).
21. Rowe, M. *et al. J. exp. Med.* **173,** 147–158 (1991).
22. Picchio, G. R. *et al. Cancer Res.* **52,** 2468-2477 (1992).
23. Janeway, C. A. Jr & Goldstein, P. *Curr. Opin. Immun.* **5,** 313–323 (1993).
24. Jenkins, M. K. & Johnson, J. G. *Curr. Opin. Immun.* **5,** 361–367 (1993).
25. Freeman, G. J. *et al. Science* **262,** 907–909 (1993).
26. Shahinian, A. *et al. Science* **261,** 609–612 (1993).
27. Duchosal, M. A. *et al. Nature* **355,** 258–262 (1992).
28. Duchosal, M. A., McConahey, P. J., Robinson, C. A. & Dixon, F. J. *J. exp. Med.* **172,** 985–988 (1990).

ACKNOWLEDGEMENTS. M.A.D. and A.L.R. contributed equally to this work. We thank M. Schapira for discussions; M. Rüegg and Ph. Trouillet for technical assistance; D. Xu for humanized mAb OKT3; G. Ambrosini for antisense oligonucleotides; the Blood Transfusion Center of Lausanne for blood products; the Pathology Institute (Miguel Gomez) of the Centre Hospitalier Universitaire Vaudois (CHUV) for performing tissue sections; and the staff of the Animal Facility of the CHUV for animal care. This work was supported by grants from the Swiss National Science Foundation (M.A.D.), the NIH (D.C.A.), an established investigatorship award from the American Heart Association (D.C.A.), and by Johnson & Johnson.

# A histone octamer-like structure within TFIID

**Alexander Hoffmann*§, Cheng-Ming Chiang*§, Thomas Oelgeschläger*, Xiaoling Xie†, Stephen, K. Burley†, Yoshihiro Nakatani‡ & Robert G. Roeder***

* Laboratory of Biochemistry and Molecular Biology, and † Laboratories of Molecular Biophysics and Howard Hughes Medical Institute, The Rockefeller University, 1230 York Avenue, New York, New York 10021, USA
‡ National Institute of Child Health and Human Development and National Institute of Neurological Disorders and Stroke, National Institutes of Health, Bethesda, Maryland 20892, USA

**THE general transcription factor TFIID nucleates initiation complex formation through direct core promoter binding[1,2], commits promoters within chromatin to transcription[3], and mediates the action of transcriptional activators, a phenomenon that may correlate with enhanced TFIID recruitment[4–7] or conformational changes in TFIID-promoter complexes[8,9]. Molecular studies of the multiprotein TFIID complex have identified a primary TATA binding subunit (TBP)[2], TBP-associated factors (TAFs) that interact with and mediate the function of activators[2,7,10,11] and intersubunit interactions[2] but have yielded relatively little insight into the structural organization of the complex or the actual mechanism of transcriptional activation. Here we present biochemical evidence for the structural relevance of histone homologies in the human TFIID subunits hTAF80, hTAF31 and hTAF20/15. Together with analyses of native TFIID complexes and accompanying crystallographic studies[12], the results suggest that there is a histone octamer-like TAF complex within TFIID.**

Our database searches with the conserved domain of recently cloned human TFIID subunits TAF20/15 (refs 13; A.H. and R.G.R., manuscript submitted) and their *Drosophila* homologues dTAF28/22 (refs 14, 15) uncovered a weak sequence similarity with histone H2B (22% identity, 56% similarity) and archaebacterial histone-like proteins (Fig. 1). This is particularly interesting in light of previously published sequence similarities between other TFIID subunits and histones H3 and H4 (refs 15,16). Alignments incorporating predictions of secondary structure emphasize the extent of the sequence relationships over the entire histone fold (Fig. 1). Comparisons of sequence identities indicate that histone-like TAF sequences have diverged from histones as long ago as the split between archaebacteria and eukaryotes, but after the presumed gene-duplication event that resulted in the histone H3 and H4 genes (data not shown).

To investigate the significance of proposed histone homologies we developed an assay that could reveal structural conservation of protein–protein interaction surfaces and that may be useful in examining the structural relevance of alleged histone relatedness of a growing number of proteins[17]. Individual histone proteins, expressed as glutathione *S*-transferase (GST) fusion proteins, were immobilized at equal concentrations (Fig. 2*a*) and used as substrates in binding assays with recombinant histones and corresponding histone-related TAFs. Each epitope-tagged histone displayed interactions (Fig. 2*b–e*) consistent with those revealed by previous biochemical and crystallographic studies with native histone complexes[18]. Thus H2A shows high-affinity binding to H2B (Fig. 2*b*, lane 4), and lower-affinity interactions with H3 and H4 (Fig. 2*b*, lanes 5, 6) that may contribute to the association of the H2A–H2B heterodimer with the H3–H4 tetramer. Reciprocally, H2B interacts strongly with immobilized H2A (Fig. 2*c*, lane 3) and more weakly with H4 (lane 6). Binding patterns observed *in vitro* with immobilized H3 (Fig. 2*d*) and immobilized H4 (Fig. 2*e*) are also similar to those observed in the native histone octamer. Although extensive biochemical studies of histones have mapped intra-octamer interactions by limited crosslinking of native histones[19], we believe that our data provide the first demonstration that these protein–protein interactions can be recapitulated with recombinant proteins. This would enable mutagenesis studies of interaction surfaces to be performed in the future.

Next, full-length epitope-tagged TAF proteins produced in bacteria (f:TAF20) or baculovirus/Sf9 cells (f:TAF31 and f:TAF80) were tested for their ability to interact with immobilized histones. TAF20 interacts strongly with histone H2A and more weakly with H4 (Fig. 2*f*), indicating that some of its protein-interaction surfaces are similar to those of histone H2B. Similarly, f:TAF31 (Fig. 2*g*) and f:TAF80 (Fig. 2*h*) display protein-interaction potentials reminiscent of histones H3 and H4, respectively. Similar assays with truncated human TAFs constructed on the

§ Present addresses: Department of Biology, Massachusetts Institute of Technology, 77 Massachusetts Avenue, Cambridge, Massachusetts 02139, USA (A.H.); Department of Biochemistry, University of Illinois at Urbana-Champaign, 600 South Mathews Avenue, Urbana, Illinois 61801, USA (C.-M.C.).

basis of sequence alignments (Fig. 1) confirmed that histone-like interaction potentials of TAF20/15, TAF31 and TAF80 are due to domains with proposed homologies to H2B (Fig. 2*i*), H3 (Fig. 2*j*) and H4 (Fig. 2*k*), respectively. These observations prompted us to initiate their biophysical characterization.

Finally, we used histone-like domains in TAFs as affinity matrices (Fig. 2*l*) to demonstrate their capacity for histone octamer-like associations with TAF20 (Fig. 2*m*), TAF31 (Fig. 2*n*) and TAF80 (Fig. 2*o*). Although no H2A-homologous TAF has been identified, we found a strong TAF20 self-association (Fig. 2*m*, lane 3) that is detected as dimer formation in gel-exclusion chromatography of recombinant TAF20/15 (data not shown). Together with crystallographic studies that have indicated an H3/H4-like heterotetramer of the *Drosophila* homologues of hTAF80/31 (ref. 12), the results presented here suggest the potential formation of a histone octamer-like TAF complex that may be described as $(hTAF20/15)_2$-(hTAF80-HTAF31)$_2$-$(hTAF20/15)_2$.

To assess the physiological significance of histone-like domains in TAFs, HeLa-derived cell lines were established that stably express the epitope-tagged H2B homology domain of TAF20/15, which, *in vitro*, mediates all observed TAF20/15 protein interactions (A.H. and R.G.R., manuscript submitted). TFIID fractions from such a cell line (hf:C109, which expresses epitope-tagged TAF20(52–161)), as well as from an epitope-tagged TBP-expressing cell line (f:TBP)[20] and the parental control HeLa cell line, were immunoprecipitated with anti-epitope antibody. Western blotting confirmed the presence of corresponding epitope-containing polypeptides in the hf:C109 and f:TBP cell line-derived immunoprecipitates but not in that from control HeLa cells (Fig. 3*a*). A similar western blot probed with antigen-purified antibodies directed against TBP and a small carboxy-terminal piece of TAF20/15 demonstrates that TBP (upper open arrow) and significant amounts of apparently full-length TAF20 and TAF15 (lower open arrows) are present, in addition to HA-FLAG-C109 (solid arrow), in the hf:C109 immunoprecipitate (Fig. 3*b*). A mixture of seven antisera specific to human TAFs was used in a third western blot to confirm that the hf:C109-derived complex is indeed a TFIID complex (Fig. 3*c*). Finally, when used in an *in vitro* transcription assay reconstituted with recombinant and highly purified general transcription factors, hf:C109-derived TFIID proved as efficient as f:TBP·IID in supporting both accurate basal and activated transcription (Fig. 3*d*).

These data demonstrate that the histone homology region in TAF20/15 is sufficient for incorporation into a functional TFIID complex, and that this domain of the protein is responsible for functionally important protein–protein interactions. Furthermore, that natural endogenous TAF20 and TAF15 polypeptides are co-precipitated with the tagged exogenous form indicates that there are multiple copies of TAF20/15 in the TFIID complex. Given a ~ 20-fold lower expression level of HA-FLAG-C109 in the hf:C109 cell line relative to endogenous TAF20/15 (data not shown), we can assume that epitope-precipitated complexes contain a single copy of the exogenous polypeptide. Phosphorimager quantification of an $^{125}$I-protein A-labelled western blot with antibodies against shared epitopes (as in Fig. 3*b*) revealed that the HA-FLAG-C109 polypeptide constitutes 22% of the total TAF20/15-related polypeptides in TFIID. This is in accordance with a four-fold stoichiometry predicted by our model of a histone octamer-like substructure within TFIID.

On the basis of present results and available protein-interaction data[13,14,16,21,22] (A.H. and R.G.R., manuscript submitted), we favour a model (Fig. 4) in which TFIID functions as a scaffold for core promoter DNA sequences that, with TFIID, constitute a docking platform for recruitment of remaining initiation factors. This model suggests some provocative hypotheses for TFIID

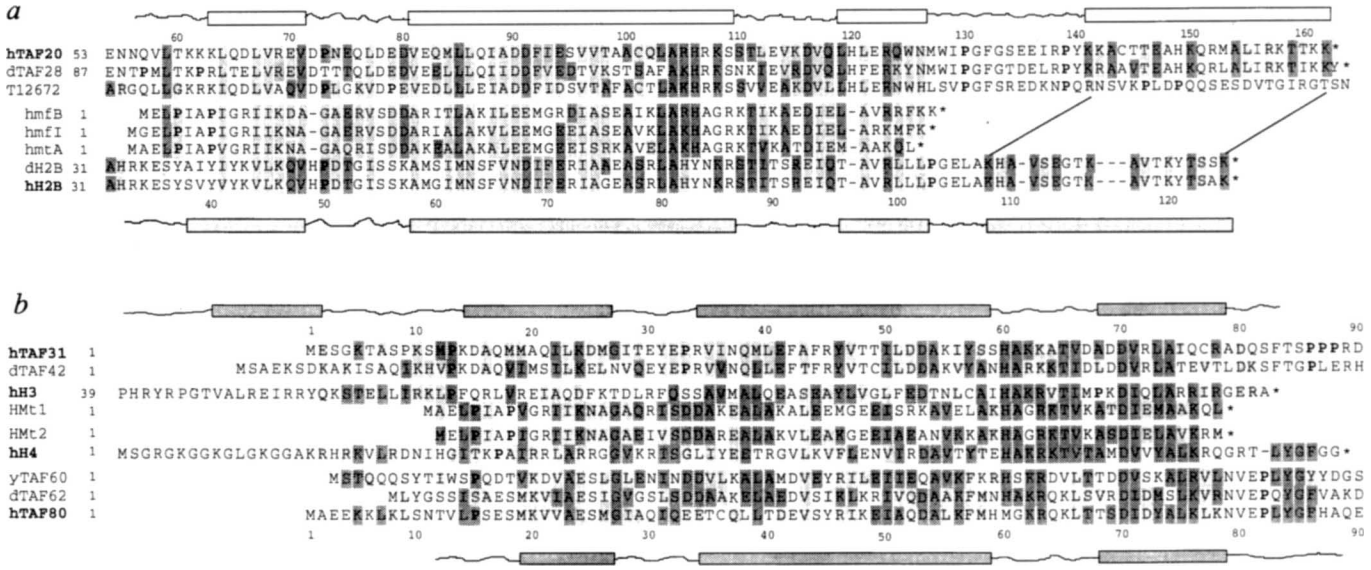


FIG. 1 Sequence similarities between TFIID subunits and histones. *a*, Sequence alignment between TAF20/15 and H2B. Alignment of partial amino-acid sequences of human TAF20/15 (A.H. and R.G.R., manuscript submitted), *Drosophila* TAF28/22 (refs 14, 15), a putative maize homologue T12672 (A.H. and R.G.R., manuscript submitted), archaebacterial histone H2B-like proteins hmfB. hmfI and hmtA, as well as *Drosophila* and human histone H2B. Residues identical between either TAFs and any of the shown histone or histone-like proteins are darkly shaded; similar residues (in the following groupings: D, E, N; E, D, Q; K, R, H; L, T; L, V, I, A, M; P, G; S, T; C, S; N, Q; F, Y) are lightly shaded; potential helix breakers (prolines) are in bold; an asterisk indicates the C terminus. Empty boxes above the sequence indicate α-helices predicted by secondary structure analysis (A.H. and R.G.R., manuscript submitted) of the hTAF20/15 and dTAF28/22 sequences; below, shaded boxes indicate α-helices identified by X-ray crystallographic analysis of the nucleosome core octamer[18]. *b*, Sequence aligment between TAF31/TAF80 and H3/H4. Partial amino-acid sequences of human TAF31 and TAF80 (ref. 16) as well as *Drosophila* TAF42 and TAF62 (ref. 15) and yeast TAF60 (ref. 29) are aligned with those of apparently related archaebacterial proteins and H3 and H4 to show their mutual interrelatedness. Residues are highlighted and secondary structure is indicated as in *a*.

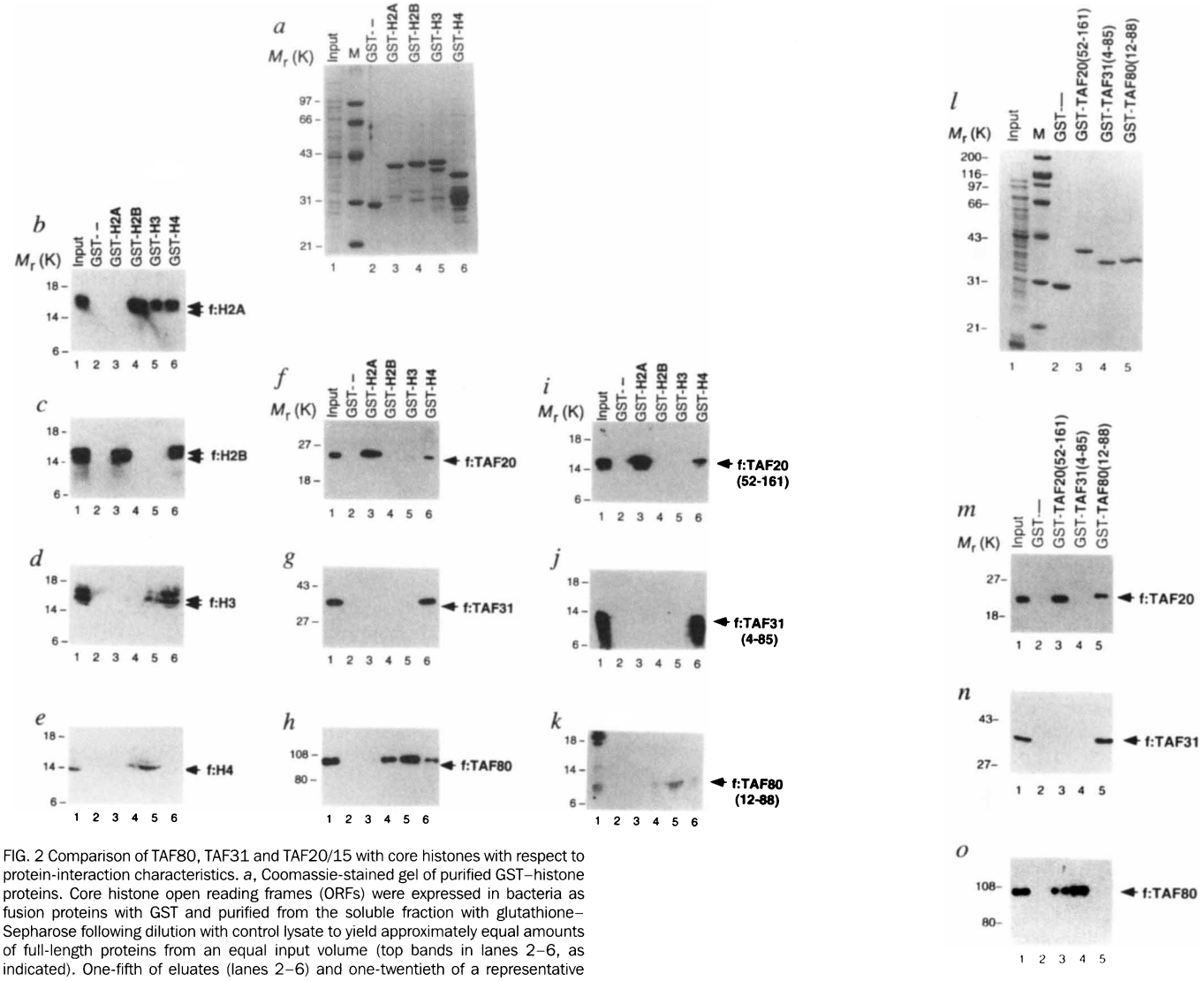


FIG. 2 Comparison of TAF80, TAF31 and TAF20/15 with core histones with respect to protein-interaction characteristics. *a*, Coomassie-stained gel of purified GST–histone proteins. Core histone open reading frames (ORFs) were expressed in bacteria as fusion proteins with GST and purified from the soluble fraction with glutathione–Sepharose following dilution with control lysate to yield approximately equal amounts of full-length proteins from an equal input volume (top bands in lanes 2–6, as indicated). One-fifth of eluates (lanes 2–6) and one-twentieth of a representative input (lane 1) are subjected to SDS–polyacylamide gel electrophoresis (PAGE) in this and all subsequent panels. *b–e*, Interaction characteristics of core histones with each other. *f–h*, Interaction characteristics of TAF20, TAF31 and TAF80 with core histones. *l–k*, Interaction characteristics of the histone-like domains in TAF20/15, TAF31 and TAF80 with core histones. *l*, Coomassie-stained gel of purified GST-fusion proteins containing histone-like domains of TAF20/15, TAF31 and TAF80. Histone-like domains defined by sequence alignments (Fig. 1) were expressed in bacteria as fusion proteins with GST and purified as above. *m–o*, Interaction characteristics of TAF20, TAF31 and TAF80 with histone-like domains in TAFs.

METHODS. Histone ORFs were generated from genomic clones[30] by polymerase chain reaction (PCR). Histone homology regions of TAF80, TAF31 and TAF20/15 were generated similarly from cDNAs[16]. These were inserted into pGEX-2TL(+)[13] and FLAG-pET11d[20] between *Nde*I and *Bam*HI sites. The expression of histone H4 was improved by optimizing codons for the bacterial translation machinery and removing 12 CpG dinucleotides. Histone homology regions of TAF80, TAF31 and TAF20 were similarly cloned into the same expression vectors. Bacterial expression and GST-interaction assays were performed with 0.5 M NaCl with 0.2% NP40 and 0.02% sarkosyl as described elsewhere (A.H. and R.G.R., manuscript submitted) and visualized by anti-FLAG tag (M2, Kodak) western analysis. Experimental procedures were identical in all parts of this figure, and all recombinant proteins were expressed in bacteria, except f:TAF31 (*g*) and f:TAF80 (*h*), which were expressed in the baculovirus/Sf9 system.

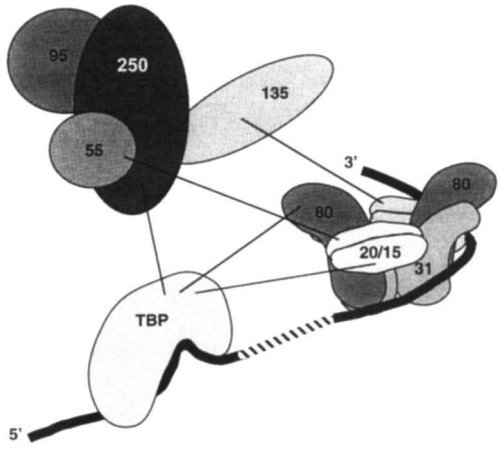


FIG. 4 A model of the TFIID complex. This exploding view of TFIID emphasizes a nucleosome-like complex consisting of TAF80, TAF31 and TAF20/15 that is tightly linked by multiple interactions[13,14,16,21,22] (A.H. and R.G.R., manuscript submitted) (indicated by lines) to TBP and co-activator TAFs (TAF250, TAF135, TAF55 and TAF95), some of which have been shown to contact activators. The DNA is represented by a thick line curving around the TAF-octamer. Smaller TAFs of unknown function and structure described previously[13] are not shown here, for clarity.

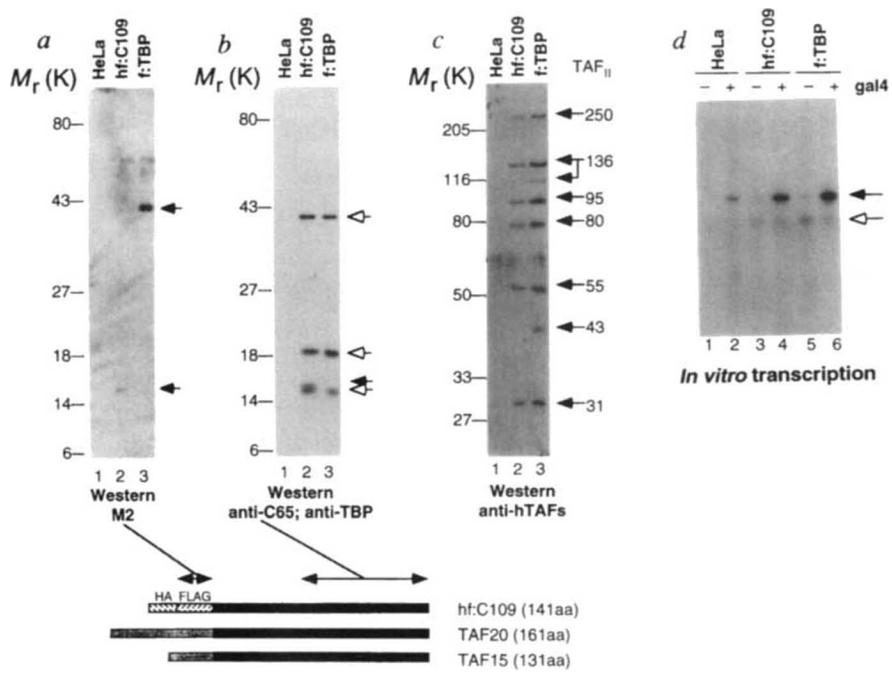


FIG. 3 Histone similarity region of TAF20/15 is sufficient for incorporation into a functional TFIID complex. *a*, Anti-FLAG western blot. Immunoprecipitates from indicated HeLa cell line-derived phosphocellulose fractions were tested for the presence of FLAG-epitope-containing proteins. The upper arrow indicates FLAG-tagged TBP (lane 3); the lower arrow indicates FLAG-tagged H2B-like domain of TAF20/15 (hf:C109, lane 2). *b*, Western blot with anti-TBP and anti-TAF20 antibodies. Immunopurified samples were tested for the presence of TBP with anti-htBP antiserum, as well as for TAF20/15 and their derivatives with antigen-purified antibodies against the C-terminal 65 amino acids of TAF20/15. Top open arrow indicates TBP, middle open arrow TAF20, and lower open arrow TAF15. Solid arrow indicates the TAF20/15 derivative hf:C109 (lane 2). *c*, Western blot with seven antisera against human TAFs. Immunopurified samples were tested for the presence of human TAFs. Antisera, each specific for a single human TAF, were first used individually and titered (data not shown) and then mixed for the purposes of this immunoblot. Arrows point at bands of indicated TAFs. *d*, *In vitro* transcription assay. Immunopurified samples were used in an *in vitro* transcription assay to test their ability to support activator-independent (basal; lanes 1, 3 and 5) and activated transcription (lanes 2, 4 and 6). The solid arrow indicates the run-off transcript form a Gal4 site-containing promoter ($pG_5HMC_2AT$); the open arrow indicates core promoter (pMLΔ53) initiated transcripts[22].

METHODS. The hf:C109 cell line was generated by retrovirus-mediated gene transfer with HA-FLAG-C109-pBABE-neo as described previously for the f:TBP cell line 3–10 (ref. 20) also used here. Nuclear extracts were prepared, fractionated on phosphocellulose and then used for immunopurification of TFIID with M2-agarose (Kodak) as described[20], using tenfold more input material for each preparation of hf:C109·IID than for f:TBP·IID. *In vitro* transcription assays were performed as described[22]. Anti-C65 serum is described elsewhere (A.H. and R.G.R., manuscript submitted).

function. Although histone 'handshake' motifs[18] within TAFs[12] may simply constitute protein-interaction domains in TFIID subunits, positive charges on the histone octamer surface lining the path of the DNA superhelix[23] are at least partly conserved in the TAFs and indicative of the possibility of TAF–DNA interactions. Indeed, early characterization of TFIID–promoter interactions likened the nuclease protection patterns of TFIID with those of nucleosomes, leading to speculations about DNA wrapping[24,25]. In addition, a protein of relative molecular mass 60,000 ($M_r$ 60K), potentially equivalent to dTAF62, was found to cross-link to downstream sequences of the *Drosophila* heat-shock protein 70 (hsp 70) promoter in a TATA-dependent manner[26]. Histone-like DNA interactions and bending may contribute to the stability of the initiation complex, and could account for the functional significance of downstream regions on weak TATA-containing[27] or TATA-less[28] promoters. Retention of TFIID components on transcriptionally inactive mitotic chromosomes (N. Segil, A.H., R.G.R. and N. Heintz, manuscript submitted) is indicative of a nucleosome-like stability of the TFIID-promoter complex within physiological chromatin. In this context, activation effects by upstream factors may be achieved through induction of conformational changes of TFIID-promoter complexes that allow more efficient formation of complete initiation complexes[8,9], rather than simply through TFIID recruitment *per se*[4–7]. □

Received 31 January; accepted 5 March 1996.

1. Roeder, R. G. *Trends biochem. Sci.* **16,** 402–408 (1991).
2. Burley, S. K. & Roeder, R. G. *A. Rev. Biochem.* (in the press).
3. Owen-Hughes, T. & Workman, J. L. *Crit. Rev. euk. Gene Express.* **4,** 403–441 (1994).
4. Abmayr, S. M., Workman, J. L. & Roeder, R. G. *Genes Dev.* **2,** 542–553 (1998).
5. Workman, J. L., Abmayr, S. M., Cromlish, W. A. & Roeder, R. G. *Cell* **55,** 211–219 (1988).
6. Lieberman, P. M. & Berk, A. J. *Genes Dev.* **8,** 995–1006 (1994).
7. Sauer, F., Hansen, S. K. & Tjian, R. *Science* **270,** 1783–1788 (1995).
8. Horikoshi, M., Hai, T., Lin, Y.-S., Green, M. R. & Roeder, R. G. *Cell* **54,** 1033–1042 (1988).
9. Horikoshi, M., Carey, M. F., Kakidani, H. & Roeder, R. G. *Cell* **54,** 665–669 (1988).
10. Chen, J.-L., Attardi, L. D., Verrijzer, C. P., Yokomori, K. & Tjian, R. *Cell* **79,** 93–105 (1994).
11. Jacq, X. *et al. Cell* **79,** 107–117 (1994).
12. Xie, X. *et al. Nature* **380,** 316–322 (1996).
13. Mengus, G. *et al. EMBO J.* **14,** 1520–1531 (1995).
14. Yokomori, K., Chen, J.-L., Admon, A., Zhou, S. & Tjian, R. *Genes Dev.* **7,** 2587–2597 (1993).
15. Kokubo, T. *et al. Nature* **367,** 484–487 (1994).
16. Hisatake, K. *et al. Proc. natn. Acad. Sci. U.S.A.* **92,** 8195–8199 (1995).
17. Baxevanis, A. D., Arents, G., Moudrianakis, E. N. & Landsman, D. *Nucleic Acids Res.* **23,** 2685–2691 (1995).
18. Arents, G., Burlingame, R. W., Wang, B.-C., Love, W. E. & Moudrianakis, E. N. *Proc. natn. Acad. Sci. U.S.A.* **88,** 10148–10152 (1991).
19. Pruss, D., Hayes, J. J. & Wolffe, A. P. *BioEssays* **17,** 1–10 (1995).
20. Chiang, C.-M., Ge, H., Wang, Z., Hoffmann, A. & Roeder, R. G. *EMBO J.* **12,** 2749–2762 (1993).
21. Thut, C. J., Chen, J.-L., Klemm, R. & Tjian, R. *Science* **267,** 100–104 (1995).
22. Chiang, C.-M. & Roeder, R. G. *Science* **267,** 531–536 (1995).
23. Arents, G. & Moudrianakis, E. N. *Proc. natn. Acad. Sci. U.S.A.* **90,** 10489–10493 (1993).
24. Sawadogo, M. & Roeder, R. G. *Cell* **43,** 165–175 (1985).
25. Nakajima, N., Horikoshi, M. & Roeder, R. G. *Molec. cell. Biol.* **8,** 4028–4040 (1988).
26. Gilmour, D. S., Dietz, T. J. & Elgin, S. C. R. *Molec. cell. Biol.* **10,** 4233–4238 (1990).
27. Nakatani, Y. *et al. Nature* **348,** 86–88 (1990).
28. Martinez, E. *et al. Proc. natn. Acad. Sci. U.S.A.* **92,** 11864–11868 (1995).
29. Poon, D. *et al. Proc. natn. Acad. Sci. U.S.A.* **92,** 8224–8228 (1995).
30. Zhong, R., Roeder, R. G. & Heintz, N. *Nucleic Acids Res.* **11,** 7409–7425 (1983).

ACKNOWLEDGEMENTS. We thank R. Takada and M. Horikoshi for anti-TAF250 and anti-TAF80; M. Guermah for anti-TAF31; S. Stevens for anti-TAF135 and the partial TAF135 cDNA; N. Heintz for histone genomic clones; and N. Segil, J. Darnell, A. Wolffe and J. Workman for discussions, encouragement and/or critical reading of the manuscript. This work was supported by a Boehringer-Ingelheim graduate fellowship (A.H.), by postdoctoral fellowships from the Helen Hay Whitney Foundation and the Aaron Diamond Foundation (C.-M.C.), the Deutsche Forschungsgemeinschaft (T.O.), by grants from the NIH and the Pew Trust to the Rockefeller University (R.G.R.), and the Howard Hughes Medical Institute (S.K.B.).

CORRESPONDENCE AND MATERIALS. Requests should be addressed to R.G.R. (e-mail address roeder@rockvax.rockefeller.edu).